BJPS

Brazilian Journal of
Pharmaceutical Sciences
vol. 52, n. 4, oct./dec., 2016
http://dx.doi.org/10.1590/S1984-82502016000400023

Article

Application of biosynthesized ZnO nanoparticles on an electrochemical H_2O_2 biosensor

Yuhong Zheng, Zhong Wang, Feng Peng, Li Fu*

[1]*Institute of Botany, Jiangsu Province and Chinese Academy of Sciences, Nanjing Botanical Garden, Mem. Sun Yat-Sen, Nanjing, China*

ZnO nanoparticles (NPs) were synthesized via a green biochemical method using *Corymbia citriodora* leaf extract as a reducing and stabilizing agent. The biosynthesized ZnO NPs were characterized by SEM and XRD. An electrochemical H_2O_2 biosensor was fabricated by modification of a glassy carbon electrode using our proposed ZnO NPs. The electrochemical sensor showed excellent detection performance towards trace amounts of H_2O_2, demonstrating that it could potentially be used in clinical applications.

Uniterms: H_2O_2/electrochemical biosensor. ZnO/biosynthesis. *Corymbia citriodora*/stabilizing agent.

INTRODUCTION

H_2O_2 is a substance that can be easily decomposed to produce free radicals, which may cause great harm to human health. In fact, H_2O_2 is widely used in various chemical processes involved in the fields of food, pharmaceuticals and the environment. Moreover, human beings also naturally produce H_2O_2 as a by-product of oxidative metabolism. Therefore, H_2O_2 determination methods have attracted considerable attention, particularly in the pharmaceutical and clinical fields. To date, numerous methods such as spectrophotometry (Regenhard, Nakov, Sauerwein, 2014), titrimetry (Klassen, Marchington, McGowan, 1994), chemiluminescence (Díaz, Sanchez, García, 1996) and chromatography (Gimeno *et al.*, 2015) have been used for the determination of H_2O_2. However, the existing methods often suffer from interference, high time cost, the use of expensive reagents and the requirement of pre-treatments. The electrochemical method, on the other hand, is faster and easier and exhibits higher selectivity and sensitivity for the determination of H_2O_2 (Chirizzi *et al.*, 2016; Zamfir *et al.*, 2016).

Commercial electrodes cannot be effectively used for H_2O_2 detection because they are limited by slow electron transfer and a high overpotential at which the reduction or oxidation of H_2O_2 occurs. One effective way to overcome this problem is to modify the electrode surface with an advanced modifier, which can decrease the overpotential and increase the kinetics of electron transfer. Many materials have been used to enhance electrochemical activity because these modifiers have large surface-to-volume ratios and high catalytic efficiency (Fu *et al.*, 2015; Zhang, Sheng, Zheng, 2015; Regenhard, Nakov, Sauerwein, 2014). Among them, nanostructured materials are attracting increasing attention due to their favorable performance in electrochemical sensors and biosensors (Chira *et al.*, 2014). For example, AuCu nanowires were prepared via a facile water solution method at room temperature and successfully used for electrochemical H_2O_2 detection (Wang *et al.*, 2015). ZnO nanoparticles were prepared and used for the deposition of horseradish peroxidase. The fabricated sensor was successfully used for the detection of H_2O_2. Most nanomaterials are prepared using chemical methods, which involve harmful reagents. Therefore, chemically prepared nanomaterials are usually not favorable for pharmaceutical and clinical applications. The biosynthesis of nanoparticles has recently attracted considerable attention due to its simplicity, low cost and nontoxicity (Zhang *et al.*, 2014). It has been shown that the metal nanoparticles produced via plant-assisted methods are more stable than those produced by other methods. Plant extracts can be used as an excellent reducing agent to provide an easy and safe green method for the scale-up and industrial production of well-dispersed metal nanoparticles (NPs). The biosynthesis of ZnO NPs using plants, including *Vitex negundo* (Ambika,

***Correspondence:** L. Fu. Institute of Botany. Jiangsu Province and Chinese Academy of Sciences. Nanjing Botanical Garden, Mem. Sun Yat-Sen. 210014 - Nanjing, China. E-mail: lifugyt@gmail.com

Sundrarajan, 2015), *Aloe vera* (Ayeshamariam *et al.*, 2014), *Pichia fermentans* (Chauhan, Reddy, Abraham, 2015), *Tribulus terrestris* (Zhao, Wang, Liu, 2015) and *Azadirachta indica* (Bhuyan *et al.*, 2015), has been reported in the literature. We also successfully synthesized ZnO NPs using *Corymbia citriodora* leaf extract and tested the particles' photocatalytic activity (Zheng *et al.*, 2015). *Corymbia citriodora* is a tall tree that grows widely in temperate and tropical northeastern Australia. Citronellal is the major chemical component of *Corymbia citriodora*, which may exert a reducing effect on certain chemicals. In this study, we explored the application of biosynthesized ZnO NPs for constructing a H_2O_2 biosensor. Because a green synthesis method was used, the fabricated electrochemical H_2O_2 sensor could potentially be used in the pharmaceutical field and in clinical tests.

Experimental

Corymbia citriodora plants were collected from a local nursery in Nanjing (Nanjing Landscape Company, No.145 Longpan Rd, Nanjing, Jiangsu), and the leaf extract was prepared as follows. In a typical experiment, 5 g of *Corymbia citriodora* leaves was washed with ultrapure water and cut into small pieces. The leaves were then boiled in 30 mL of ultrapure water for 15 min. After cooling, the leaf extract was filtered, centrifuged and stored in a refrigerator. Zinc nitrate hexahydrate ($Zn(NO_3)_2 \cdot 6H_2O$), ammonium hydroxide (28–30%NH_3 basis), H_2O_2, ascorbic acid, uric acid and glucose were purchased from Sigma-Aldrich. All other chemicals used were analytical grade reagents and were employed without further purification. Ultrapure water was used in all experiments.

The method for the biosynthesis of ZnO NPs was reported in our previous study. In a typical experiment, 20 mL *Corymbia citriodora* leaf extract was added to a 0.5 M zinc nitrate solution (2:5 wt%) and continuously stirred at 80 °C for 48 h. A pale white precipitate was obtained through centrifugation and washed with methanol and ultrapure water. The ZnO NPs were then collected after dried in an oven overnight. Chemically synthesized ZnO NPs were prepared using a similar method in which ammonium hydroxide was used instead of the *Corymbia citriodora* leaf extract.

The crystal phase information of the sample was characterized at Bragg angles (2θ) ranging from 5° to 80° by X-ray diffraction (XRD) with Cu Kα radiation (D8-Advanced, Bruker, Germany). The average crystal size was calculated using the Debye–Scherrer equation:

$$D = \frac{0.9\lambda}{B\cos\theta}$$

where D is the average crystal size, λ is the wavelength of X-rays, B is the full width at half maximum and θ is the diffraction angle.

The surface morphology of the ZnO NPs was characterized by scanning electron microscopy (SEM, ZEISS SUPRA 40VP combined with EDX, Germany).

For electrochemical experiments, a glassy carbon electrode (GCE) was polished with an alumina-water slurry, followed by rinsing with ethanol and ultrapure water. To modify the electrode surface, a certain amount of a nanocomposite dispersion (1 mg/mL) was dropped onto the GCE and dried at room temperature. Electrochemical measurements were performed on a CH Instruments 660A electrochemical workstation (CH Instruments, Texas, USA) using a three-electrode system. A platinum wire was used as the auxiliary electrode and Ag/AgCl (3 M KCl) as the reference electrode.

RESULTS AND DISCUSSION

Figure 1 shows an SEM image of biosynthesized ZnO NPs. The figure shows that the ZnO NPs reduced by *Corymbia citriodora* leaf extract were well dispersed. No distinct aggregation was observed by SEM characterization. This excellent dispersibility could be due to the adsorption of organic compounds on the surface of the ZnO NPs from *Corymbia citriodora,* which provides sufficient surface charge between individual ZnO NPs. The excellent dispersibility of the ZnO NPs could provide a higher surface area, which could benefit the adsorption of target molecules during electrochemical testing. The average particle size of the biosynthesized ZnO NPs was determined to be 47 nm based on the measurement of 300 individual ZnO NPs. The formation of ZnO NPs was confirmed by XRD analysis. As shown in Figure 2A, the XRD pattern of the biosynthesized showed peaks at 31.7°, 34.6°, 36.3°, 47.5°, 56.3°, 62.9° and 68.0°, which can be indexed to hexagonal wurtzite ZnO (JCPDS 36-1451) and match the peaks associated with chemically reduced ZnO (Figure 2B). The average crystallite size of the biosynthesized ZnO NPs was calculated to 21.7 nm using the Debye–Scherrer equation.

The electrochemical behavior of the biosynthesized ZnO (B-ZnO) modified GCE, chemically synthesized ZnO (C-ZnO) modified GCE and bare GCE were studied by electrochemical impedance spectroscopy (EIS). Two types of result from the EIS measurements

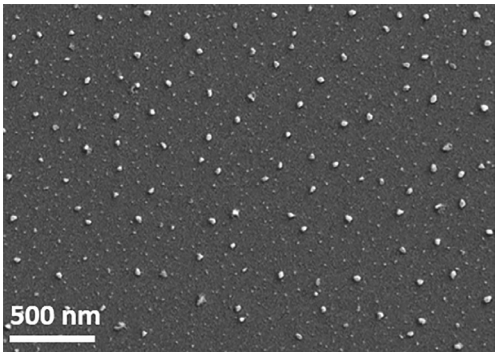

FIGURE 1 - Scanning electron microscopy image of biosynthesized ZnO nanoparticles using *Corymbia citriodora* leaf extract.

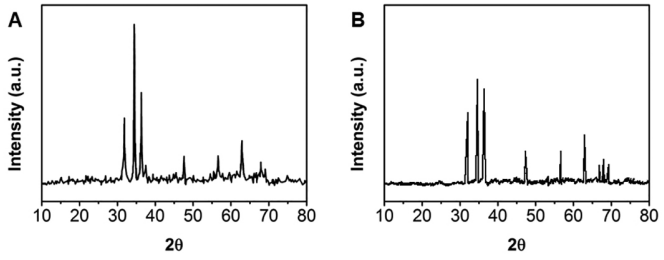

FIGURE 2 - X-ray diffraction pattern of (A) biosynthesized ZnO nanoparticles and (B) chemically synthesized ZnO.

can be expected from a typical Z' (real part) versus Z'' (imaginary part) resistance plot. A semicircular graph is often observed at higher frequencies, which is attributed to electron-transfer-limited processes at the electrode surface. The second type of plot is linear and commonly occurs at lower frequencies. This plot is related to diffusion-limited processes at the electrode surface. In the former case, the diameter of the semicircular plot is proportional to the electron-transfer resistance. As shown in Figure 3, the bare GCE displayed a larger semicircle compared with that of the modified GCE, indicating that the bare GCE exhibited higher electron-transfer resistance. The EIS of C-ZnO/GCE showed a slightly smaller semicircle, indicating the C-ZnO could lower the electron-transfer resistance. Moreover, the B-ZnO/GCE showed a much smaller semicircle, suggesting that the biosynthesized ZnO could effectively reduce the electron-transfer resistance at the electrode surface. Results suggest that the B-ZnO/GCE could exhibit a higher current response when interacting with target molecules.

Figure 4 shows cyclic voltammograms (CVs) for the reduction of 0.05 mM H_2O_2 at the bare GCE (curve a), C-ZnO/GCE (curve b) and B-ZnO/GCE (curve c). No obvious reduction peak was observed for the bare GCE.

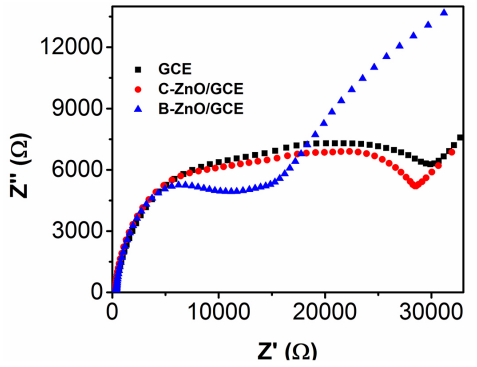

FIGURE 3 - Electrochemical impedance spectroscopy (EIS) of bare glassy carbon electrode (GCE), C-ZnO/GCE and B-ZnO/GCE in a solution containing 5 mM $[Fe(CN)_6]^{-3/-4}$+0.1 M KCl.

In contrast, a well-defined reduction peak with a peak potential at ─0.44 V was observed for C-ZnO/GCE due to the catalytic activity of ZnO NPs. Moreover, the B-ZnO/GCE presented superior electrocatalytic performance towards H_2O_2, with a higher current response and lower overpotential. The enhancement of the current response and the decrease in the overpotential of H_2O_2 reduction on the B-ZnO/GCE could be ascribed to the high specific surface area and the excellent electrocatalytic properties of the biosynthesized ZnO NPs. It has been reported that the electroreduction of H_2O_2 on ZnO NPs involves a rate-limiting chemical step followed by an electron-transfer step. The reaction can be expressed as follows:

$$H_2O_2 \rightarrow 2OH^{\bullet}_{ads}$$
$$OH^{\bullet}_{ads} + e^- \rightarrow OH^-$$

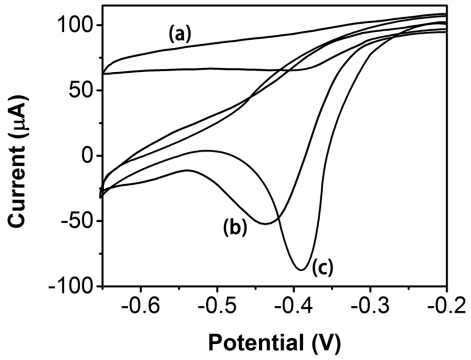

FIGURE 4 - Cyclic voltammetry results of (a) GCE, (b) C-ZnO/GCE and (c) B-ZnO/GCE towards the detection 0.05 mM H_2O_2 in PBS solution. Scan rate: 50 mV/s.

For the amperometric determination of H_2O_2, the prepared B-ZnO/GEC was evaluated by measuring the current response at a fixed potential with the addition of H_2O_2. Figure 5 shows the typical amperometric response

upon the successive addition of H_2O_2 at B-ZnO/GEC. The results indicate that the B-ZnO/GEC attained a steady-state current within 3 s, suggesting that the fabricated sensor responds rapidly to H_2O_2. A linear relationship between the current response and H_2O_2 concentration was observed between 0.1 and 150 ***μM*** (inset of B-ZnO/GCE). The corresponding linear regression equation can be expressed as follows: I (μA) = -2.0199(μM) – 1.0223 (R^2 = 0.9982). The detection limit was calculated to be 0.07 μM (S/N = 3).

The reproducibility of the proposed H_2O_2 electrochemical sensor was tested by detecting 0.05 mM H_2O_2 using six B-ZnO/GCEs. The current responses showed an acceptable relative standard deviation (RSD) of 3.1%. The stability of the proposed H_2O_2 electrochemical sensor was tested over 3000 s by a continuous I-T test in 0.05 mM H_2O_2. The responses showed a decrease of 3% in the current response. To evaluate the long-term storage stability of the sensor, the B-ZnO/GCE was tested by storing it in a refrigerator for 1 month. The current response showed that the B-ZnO/GCE retained more than 93% of its original activity. Therefore, the H_2O_2 electrochemical sensor constructed using a GCE modified with biosynthesized ZnO NPs exhibits satisfactory stability and reproducibility.

Uric acid (UA), ascorbic acid (AA) and glucose are three electro-active molecules that commonly co-exist in biological systems and could interfere with the electrochemical determination of H_2O_2. The ability to distinguish these common interfering species from the target molecule is highly important in developing a sensor. Figure 6 shows the typical amperometric response of B-ZnO/GCE upon the addition of H_2O_2 and a series of potentially interfering species, including DA, UA and glucose. A well-defined current response was observed after the addition of H_2O_2. In contrast, a 20-fold excess of UA, AA and glucose produced negligible current responses under these conditions, suggesting that the B-ZnO/GCE presents an excellent ability to detect H_2O_2 among interfering species.

The reliability of the proposed B-ZnO/GCE H_2O_2 electrochemical sensor under real-world conditions was tested using commercial toothpaste as a sample. In a typical experiment, 0.5 g toothpaste was dispersed in 20 mL ultrapure water. The dispersion was centrifuged to remove sediments and then diluted for analysis. Detection was conducted at ─0.39 V in 5 mL pH 7.0 PBS with 5 μL diluted toothpaste solution injected. The standard addition method was used for the quantitative determination. Table I shows the sample test results, which indicate that our proposed B-ZnO/GCE H_2O_2 electrochemical sensor could be reliably used to analyse real samples.

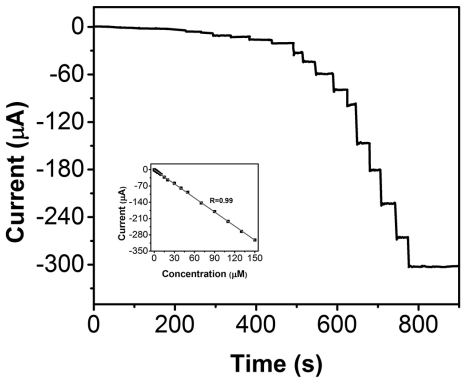

FIGURE 5 - Amperometric response of the B-ZnO/GCE with successive addition of H_2O_2 to PBS. Measured at ─0.39 V. Inset: \ plot of Ipa versus H_2O_2 concentration.

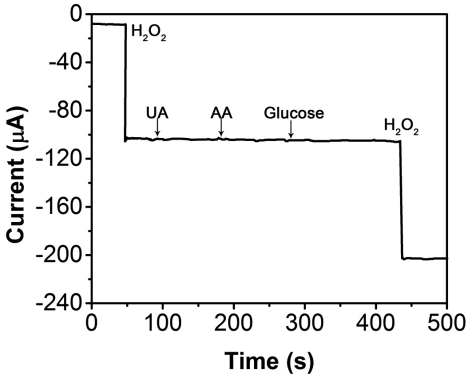

FIGURE 6 - Amperometric current response of B-ZnO/GCE to the addition of 0.05 mM H_2O_2, 1 mM uric acid (UA), 1 mM ascorbic acid (AA), 1 mM glucose and 0.05 mM H_2O_2 at an operating potential of - 0.39 V.

TABLE I - Real sample test results of determination for H_2O_2 in toothpastes

Sample	Amount detection (μM)	Amount added (μM)	Recovery (%)	RSD (%)
1	4.77	0	─	3.21
2	9.66	5	98.87	2.83
3	15.02	10	101.69	3.69
4	24.89	20	100.48	4.03

CONCLUSION

In this work, we proposed an electrochemical H_2O_2 sensor based on green biosynthesized ZnO NPs using *Corymbia citriodora* leaf extract as a reducing and stabilizing agent. The sensor exhibited a stronger ability to reduce H_2O_2 compared with that of a bare GCE and a GCE modified with chemically synthesized ZnO NPs. The results indicate that biosynthesized nanomaterials could be excellent candidates for electrochemical applications. Due to their green synthesis route and outstanding properties, biosynthesized nanomaterials are recommended for use in the pharmaceutical field and in clinical tests.

REFERENCE

AMBIKA, S.; SUNDRARAJAN, M. Green biosynthesis of ZnO nanoparticles using Vitex negundo L. extract: Spectroscopic investigation of interaction between ZnO nanoparticles and human serum albumin. *J. Photoch. Photobio. B,* v.149, p.143-148, 2015.

AYESHAMARIAM, A.; KASHIF, M.; VIDHYA, V.; SANKARACHARYULU, M.; SWAMINATHAN, V.; BOUOUDINA, M.; JAYACHANDRAN, M. Biosynthesis of (ZnO-Aloe vera) nanocoposites and antibacterial/ anifungal studies. *J. Opto. Bio. Mat.,* v.6, n.3**,** p.85-99, 2014.

BHUYAN, T.; MISHRA, K.; KHANUJA, M.; PRASAD, R.; VARMA, A. Biosynthesis of zinc oxide nanoparticles from Azadirachta indica for antibacterial and photocatalytic applications. *Mat. Sci. Semicon. Proc.,* v.32, p.55-61, 2015.

CHAUHAN, R.; REDDY, A.; ABRAHAM, J. Biosynthesis of silver and zinc oxide nanoparticles using Pichia fermentans JA2 and their antimicrobial property. *Appl. Nanosci.,* v.5, n.1**,** p.63-71, 2015.

CHIRA, A.; BUCUR, B.; RADULESCU, M.-C.; GALAON, T.; RADU, G.-L. Study of electrochemically modified electrode with synthesized N-benzyl-4, 4'-bipyridine with anti-Fouling properties for oxygen and hydrogen peroxide detection. *Int. J. Electrochem. Sc.,* v.9, p.4493-4511, 2014.

CHIRIZZI, D.; GUASCITO, M.R.; FILIPPO, E.; MALITESTA, C.; TEPORE, A. A novel nonenzymatic amperometric hydrogen peroxide sensor based on CuO@ Cu 2 O nanowires embedded into poly (vinyl alcohol). *Talanta,* v.147, p.124-131, 2016.

DÍAZ, A.N.; SANCHEZ, F.G.; GARCÍA, J.G. Hydrogen peroxide assay by using enhanced chemiluminescence of the luminol-H 2 O 2-horseradish peroxidase system: comparative studies. *Anal. Chim. Acta.,* v.327, n.2**,** p.161-165, 1996.

FU, L.; ZHENG, Y.; WANG, A.; CAI, W.; LIN, H. Sensitive determination of quinoline yellow using poly (diallyldimethylammonium chloride) functionalized reduced graphene oxide modified grassy carbon electrode. *Food Chem.,* v.181, p.127-132, 2015.

GIMENO, P.; BOUSQUET, C.; LASSU, N.; MAGGIO, A.-F.; CIVADE, C.; BRENIER, C.; LEMPEREUR, L. High-performance liquid chromatography method for the determination of hydrogen peroxide present or released in teeth bleaching kits and hair cosmetic products. *J. Pharm. Biomed. Anal.,* v.107, p.386-393, 2015.

KLASSEN, N.V.; MARCHINGTON, D.; MCGOWAN, H.C. H_2O_2 determination by the I3-method and by $KMnO_4$ titration. *Anal. Chem.,* v.66, n.18**,** p.2921-2925, 1994.

REGENHARD, P.; NAKOV, D.; SAUERWEIN, H. Applicability of a spectrophotometric method for assessment of oxidative stress in poultry. *Mace. Vet. Rev.,* v.37, n.1**,** p.43-47, 2014.

SOTOMA, S.; IGARASHI, R.; IIMURA, J.; KUMIYA, Y.; TOCHIO, H.; HARADA, Y.; SHIRAKAWA, M. Suppression of nonspecific protein–nanodiamond adsorption enabling specific targeting of nanodiamonds to biomolecules of interest. *Chem. Lett.,* v.44, n.3**,** p.354-356, 2015.

WANG, H.; JIANG, T.; XING, M.-M.; FU, Y.; PENG, Y.; LUO, X.-X. Preparation of highly crystallized yttrium oxysulfide suspension via a novel colloidal processing. *J. Nanosci. Nanotech.,* v.16, n.4**,** p.3951-3955, 2016.

WANG, N.; HAN, Y.; XU, Y.; GAO, C.; CAO, X. Detection of H_2O_2 at the nanomolar level by electrode modified with ultrathin AuCu nanowires. *Anal. Chem.,* v.87, n.1**,** p.457-463, 2015.

ZAMFIR, L.-G.; ROTARIU, L.; MARINESCU, V. E.; SIMELANE, X. T.; BAKER, P. G.; IWUOHA, E. I.; BALA, C. Non-enzymatic polyamic acid sensors for hydrogen peroxide detection. *Sensors Actuators B: Chem.,* v.226, p.525-533, 2016.

ZHANG, S.; SHENG, Q.; ZHENG, J. Synthesis of Ag-HNTs-MnO 2 nanocomposites and their application for nonenzymatic hydrogen peroxide electrochemical sensing. *RSC Adv.,* v.5, n.34**,** p.26878-26885, 2015.

ZHANG, W.; GUO, C.; CHANG, Y.; WU, F.; DING, S. Immobilization of horseradish peroxidase on zinc oxide nanorods grown directly on electrodes for hydrogen peroxide sensing. *Monatsh. Chem.,* v.145, n.1**,** p.107-112, 2014.

ZHAO, Z.-Y.; WANG, M.-H.; LIU, T.-T. Tribulus terrestris leaf extract assisted green synthesis and gas sensing properties of Ag-coated ZnO nanoparticles. *Mater. Lett.,* v.158, p.274-277, 2015.

ZHENG, Y.; FU, L.; HAN, F.; WANG, A.; CAI, W.; YU, J.; YANG, J.; PENG, F. Green biosynthesis and characterization of zinc oxide nanoparticles using *Corymbia citriodora* leaf extract and their photocatalytic activity. *Green. Chem. Lett. Rew.,* v.8, n.2**,** p.59-63, 2015.

Received for publication on 18th November 2015
Accepted for publication on 27th September 2016